Theoretical Understanding of How Solution Properties Govern Nanofiltration Performances

Sébastien Déon[1,*], Patrick Dutournié[2], Patrick Fievet[1] and Lionel Limousy[2]

[1]*Institut UTINAM (UMR CNRS 6213), Université de Bourgogne-Franche-Comté, 16 route de Gray, 25030 Besançon cedex, France*

[2]*Institut de Science des Matériaux de Mulhouse (IS2M-UMR CNRS 7361), Université de Haute-Alsace, 15 rue Jean Starcky, 68057 Mulhouse, France*

Abstract: Mechanisms governing transfer of ions through nanofiltration membranes are complex and it is primordial to understand how rejection and selectivity performances depend on the properties of the solution. For this purpose, a knowledge model based on a coupling between equilibrium partitioning induced by steric, electric and dielectric exclusions and transport inside pores by diffusion, convection and electro-migration is proposed to theoretically discuss the influence of solution properties on performances. After detailing the physical description of this model, the influence of ion size on rejection is firstly discussed from simulations obtained in several appropriate cases. Since electrostatic interactions are known to play a role on ion rejection, the influence of ion valence and concentration is then studied and different behaviors are brought to light depending on ions considered. Finally, the influence of confinement within nanopores on water dielectric properties and its consequences for ion separation are also addressed.

Keywords: Nanofiltration, Transport modelling, Physico-chemical properties, Ion rejection, Equilibrium partitioning.

1. INTRODUCTION

Nowadays, nanofiltration (NF) is recognized as an efficient technology to treat industrial or urban wastewater for purification or concentration purposes. Indeed, the specific membrane materials endow them with size and electric properties that allow high rejection performances for ions or small charged solutes while maintaining reasonable permeation flux (or applied pressures) compared to reverse osmosis dense membranes. For this reason, NF is often considered as an attractive option for the decontamination of industrial effluents from chemical, wood, food, textile or metal industries [1-4]. To investigate the reliability of a NF process for a given application, preliminary experiments are often carried out with lab-scale equipment, which can be time and money-consuming. The use of a numerical tool that can predict the flux and ion rejection performances of different membranes and especially the best experimental conditions in terms of applied pressure, feed flow-rate or temperature, would be breakthrough in the optimization steps for the development of NF processes at the industrial scale. Moreover, a numerical model based on a physical description of transport phenomena is of prime importance to understand and explain trends obtained during filtration of salts or ion mixtures [5]. The aim of this paper is to discuss how the properties of the various components of a solution as well as those of the membrane material lead to filtration performances through a series of specific theoretical cases. Numerical rejections provided by the model will allow a better understanding of the various physical mechanisms that govern the transfer of ions through the membrane and especially the interactions between charged species and membrane surface. Several physical approaches are available in literature [6-8] sbut the model used in this study is based on the coupling between ion transport inside the membrane nanopores and the equilibrium partitioning at the membrane-solution interfaces. This approach is currently used in literature and has proved its ability to describe experimental performances [9-13]. Hereafter, the knowledge model is firstly briefly described for a better understanding of physical mechanisms that are considered in this study. Then, the model is used to simulate some “ideal” case studies so as to discuss how separation performances are governed by the interaction between membrane and the various components of the filtered solution.

2. TRANSPORT MODELLING

2.1. Transport Through Membrane Pores

Various approaches were proposed to describe the transport of ions through NF membranes. Among them, the electro-kinetic approach, which was initiated in the 1960s by Gross and Osterle [14] and Dresner [15], has demonstrated its reliability. This model originally known as Space Charge Model was intensively investigated,

---

[*] Address correspondence to this author at the Institut UTINAM (UMR CNRS 6213), Université de Bourgogne-Franche-Comté, 16 route de Gray, 25030 Besançon cedex, France; Tel: (+33) 3 63 08 25 81;
Fax: (+33) 3 81 66 62 88; E-mail: sebastien.deon@univ-fcomte.fr

E-ISSN: 2410-1869/16

notably through the various simplifications and improvement made in the last decades. Nowadays, the model relying upon Schlogl's works[16]considers that the molar flux of an ion through membrane pores can be expressed by the extended Nernst-Planck (ENP) equation. The model was finally improved to bring it much closer to physical reality by including hydrodynamic coefficients $K_{i,d}$ and $K_{i,c}$ that take influence of pore wall on diffusion and convection into account.

$$\vec{j_i} = -c_i K_{i,d} D_i \vec{\nabla}\left(ln\,\gamma_i\right) - K_{i,d} D_i \vec{\nabla} c_i - \frac{z_i c_i K_{i,d} D_i}{RT} F \vec{\nabla}\psi + K_{i,c} c_i \vec{V} \tag{1}$$

Where γ_i, D_i, and c_i denote the activity coefficient, diffusivity and concentration of an ion i. V and ψ represent the solvent velocity and electric potential.

Several expressions are provided in literature to calculate the hydrodynamic coefficients [17-19] from the solute to pore size ratio λ_i [20]. Expressions proposed by Bowen and Sharif [21] were considered in this study.

$$K_{i,c} = (2-\phi_i)(1+0{,}054\lambda_i - 0{,}988\lambda_i^2 - 0{,}441\lambda_i^3) \tag{2a}$$

$$K_{i,d} = 1 - 2{,}30\lambda_i + 1{,}154\lambda_i^2 + 0{,}224\lambda_i^3 \tag{2b}$$

With ϕ_i the steric partitioning coefficient defined by Eq. 3:

$$\phi_i = \left(1-\lambda_i\right)^2 = \left(1-\frac{r_i}{r_p}\right)^2 \tag{3}$$

The molar flux can be calculated from the conservation of the species i through:

$$j_i = VC_{i,p} \tag{4}$$

with $C_{i,p}$ the concentration of ion i in the permeate solution.

Additionally, the volume permeation flux J_v can be calculated by the Darcy's law:

$$J_v = \frac{L_p}{\eta}\left(\Delta P - \Delta\pi\right) = \frac{\left(\Delta P - \Delta\pi\right)}{\eta R_m} \tag{5}$$

where η is the dynamic viscosity of solution, L_p the membrane hydraulic permeability, R_m the hydraulic resistance ($L_p = 1/R_m$) and $\Delta\pi$ the osmotic pressure difference.

2.2. Transfer at the Interfaces

The concentrations at the pore inlet and outlet that are required to solve transport through pores can be calculated by considering the equilibrium partitioning at the two-membrane/solution interfaces. The most physico-chemically detailed expression to calculate the pore to solution concentrations ratio results from the equality of generalized chemical potentials on both sides of the interface:

$$\frac{c_i}{C_i} = \frac{\gamma_{i,sol}}{\gamma_{i,pore}} \phi_i \, exp\left(-\Delta W_i\right) exp\left(\frac{-z_i F}{RT}\Delta\psi_D\right) \tag{6}$$

Where $\Delta\psi_D$ denotes the so-called Donnan potential from Donnan equilibrium theory [22] ΔWi corresponds to the energy barrier to solvation of ions into the pores, which can be expressed by the model of ion solvation energy (Eq. 7) developed by Born [23] and initially used by Guzman-Garcia *et al.* [24] in studies dedicated to ion-exchange membranes.

$$\Delta W_{i,born} = \frac{z_i^2 e^2}{8\pi\varepsilon_0 kTr_i}\left(\frac{1}{\varepsilon_p} - \frac{1}{\varepsilon_b}\right) \tag{7}$$

The numerical resolution of previous equations is reached by an iterative method and the procedure is more accurately detailed in previous papers. Briefly, permeate concentrations are firstly initialized to calculate the concentration profiles within the pore and the new permeate concentrations are calculated by means of equilibrium partitioning. These concentrations are considered for the next step after relaxation. This procedure is reiterated until convergence, that means until permeate concentration does not vary from an iteration to another. Finally, rejection is calculated from concentration in retentate and permeate streams:

$$R_i = 1 - \frac{C_{i,p}}{C_{i,r}} \tag{8}$$

To conclude this physical description of ion transport through the membrane, it should be noted that the description of multi-component rejection requires the knowledge of four physical parameters, viz. the membrane hydraulic permeability (L_p), the mean pore radius (r_p), the dielectric constant of the solution confined in nanopores (ε_p) and the membrane charge (X_d). Obviously, the physico-chemical properties of the solution and especially those of the various components also govern the filtration performances and this study is hence devoted to the link between solution properties and filtration performances.

3. INFLUENCE OF SOLUTION PROPERTIES ON REJECTION

Simulation results provided in this study represent descriptions of ideal cases so as to examine the influence of some physico-chemical parameters of the solution on the rejection performances. The values of model input parameters are arbitrarily set at classical values obtained during previous parameter identification. The values are given in Table **1**.

3.1. Influence of the Ion Size

First, it is essential to understand that ion size can be characterized by various kinds of radii, such as bare radius, hydrated radius or Stokes radius. Bare radius corresponds to the real size of the ion without considering solvation, whereas hydrated radius corresponds to the ions and its solvation sphere. Finally, Stokes radius is a hydrodynamic property defined as the radius of a hard sphere that diffuses at the same velocity as that ion. Although the bare ion radius was initially used in Born relation, the Stokes radius was also chosen as it was previously proposed by Bowen *et al*. in the Donnan-Steric Pore Model (DSPM). The influence of ion size on the rejection of salts with monovalent cations and anions is depicted in Figure **1** for salt concentrations of 100 mol m^{-3}. The various ion sizes used for simulations are collected from literature [25] and summarized in Table **2**. From Figure **1**, it can be seen that rejections predicted by considering hydrated ion radii are noticeably higher than those obtained by considering other size definitions since the radii are between 2 and 6 times higher. This trend can lead to unrealistic high rejections, especially for divalent ions that are strongly larger and hydrated. Consequently, it seems that hydrated radius is probably not the most adequate definition to describe steric partitioning at interfaces. Additionally, it can be seen in Figure **1** that generally the larger the ion size, the higher rejection is. This fact is only contradicted by rejections of cations when bare ion size is considered. Indeed, lithium rejection was found to be the highest whereas it exhibits the smaller size. Indeed, transfer is governed by steric effects at the pore inlet and outlet but by diffusion as well. In this case, small diffusivity of Li^+ balances its small size, leading to higher rejection compared with ions exhibiting higher diffusivity.

The trends obtained may seem obvious but they highlight the need to know accurately the ion size for a suitable description of ion rejection. It is difficult to conclude about the most adequate size definition to describe ion rejection since steric exclusion is never the sole mechanism that acts on rejection. As an example, sequences obtained for anions predicted with Stokes and hydrated radii seem to be in accordance with that obtained by Dutournié *et al*. [26] with an ionic mixture, contrary to the sequence predicted with bare ions, but comparison between experimental and theoretical sequences does not allow a definitive conclusion about the best size definition.

In any case, a better description could perhaps be achieved by using different definitions depending on the physical mechanism considered. Indeed, it is likely

Table 1: Values of the Various Parameters Considered in this Study

Input Parameters	Applied Pressure	Membrane Permeability	Mean Pore Radius	Membrane Charge Density	Dielectric Constant Inside Pores
	ΔP (bar)	L_p (m)	r_p (nm)	X_d (mol m^{-3})	ε_p (-)
Chosen values	0-26	2 10^{-14}	0.5	-10	60 (50-70)*

* Values in brackets are those used only in §3.4

Table 2: Values of the Various Types of Radius to Describe Monovalent Ion Size

	Anions			Cations		
Ions	Cl^-	F^-	Br^-	Na^+	K^+	Li^+
Stokes radii (nm)	0.121	0.166	0.117	0.184	0.126	0.239
Bare ion radii (nm)	0.181	0.136	0.196	0.095	0.133	0.060
Hydrated radii (nm)	0.332	0.352	0.330	0.358	0.331	0.382

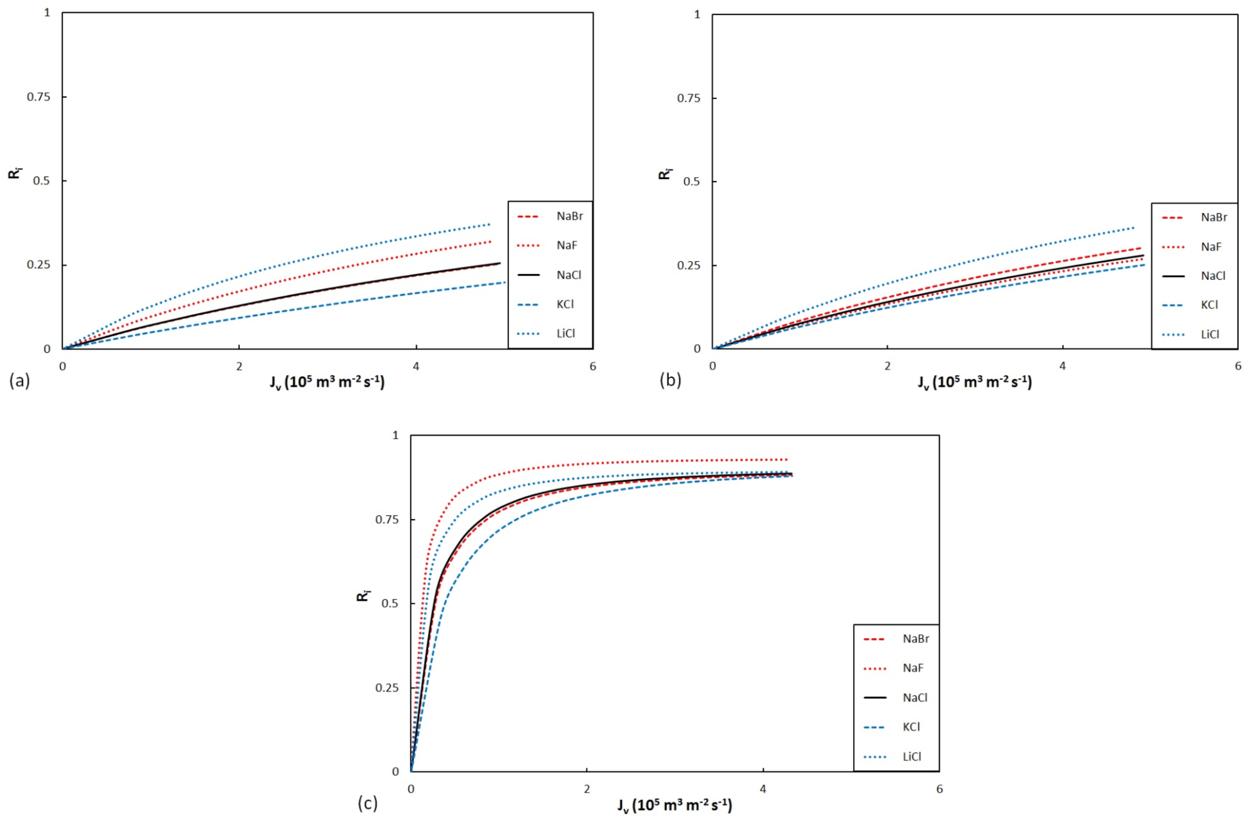

Figure 1: Evolution of salt rejection with permeation flux numerically obtained for various definitions of ion size, namely Stokes radius (**1a**), bare ion radius (**1b**) and hydrated ion radius (**1c**).

that the best definition to model interface partitioning is not necessarily the best definition to model steric hindrance for diffusion or convection. For instance, it would be more relevant to consider Stokes radii to model hindrance in transport equation even if bare radii are considered in the interface partitioning.

It is noteworthy that the steric mechanisms (partitioning and steric hindrance) are governed by the ratio between ion radius and mean pore radius, which means that an error on the ion size can be partially balanced by a variation of the mean pore size and vice-versa. However, the knowledge of ion size becomes all the more important for ionic mixtures for which separation selectivity is notably governed by the size difference between the various ions. It can be noticed from Table **2** that the ion size order differs depending on the definition used, so that the choice of the size definition can lead to major repercussions on the selectivity between ions and thus, on the performances of a separation process. Following simulations will be obtained by considering Stokes radii as ion size.

3.2. Influence of the Ion Valence

Equations mentioned in the theoretical model description clearly show that the ion valence appears in all equations, whether in equilibrium partitioning or transport inside pores. In this part, the impact of ion valence is investigated by considering virtual ions having the same size but different valences. A size of 0.15 nm and a diffusivity of 1.5 10^{-9} m^2 s^{-1} were arbitrarily chosen for all anions and cations so that only ion valence influence can be investigated. The salt rejection evolution with permeation flux for various anion and cation valences is drawn in Figure **2**.

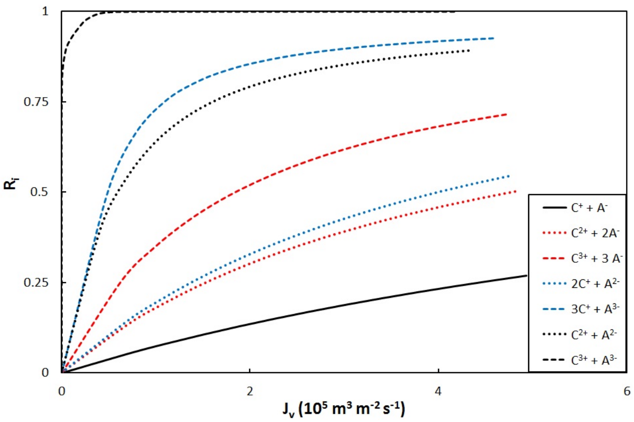

Figure 2: Evolution of salt rejection with permeation flux for various anion and cation valences numerically obtained for a negative membrane charge and a "one-size-fits-all".

From Figure **2**, it appears that the ion valence has a great impact on salt rejection due to electrostatic interactions between ions and membrane fixed charge. The higher the ion valence, the more strongly the salt is rejected. This observation is all the more true when the valence of the co-ion (in view of membrane charge) is high. Indeed, the salt rejection was found to be much higher when the co-ion (viz. cation with the negatively charged membrane considered) is trivalent than when it is the counter-ion. It can also be concluded that highest rejection is obtained when both cation and anion exhibit the highest valence. Finally, it should be noted that the opposite behavior would be obtained by considering a positively charged membrane, *i.e.* valence of cation would have a stronger influence on the rejection.

It is worthwhile to mention that the presence of one or several multivalent ions in an ion mixture strongly affects the rejection of monovalent ions due to its high rejection and can even lead to negative rejections. The influence of a divalent cation and anion in ternary mixtures can be observed in Figure **3**. It is clearly viewable in this figure that a divalent co-ion has a greater impact on monovalent ions than a divalent counter-ion since its rejection is higher, which lead to a better selectivity between the various ions.

Observations that were obtained with a single ion size and diffusivity could be all the more outstanding with “real” ions since multivalent ions usually exhibit larger size and lower diffusivity, which tends to strongly increase their rejection and their impact on other ions. Besides, such a behavior has already been observed experimentally with ternary ion mixtures containing sulfate or magnesium ions [27-29].

3.3. Influence of Concentration

It is admitted that electrostatic interactions between ions and membrane fixed charge play a primordial role on ion rejection. Since electrostatic interactions are known to depend on ion concentration, the latter should have an influence on separation performances. The influence of salt concentration on its rejection for a constant charge density X_d (-10 mol m^{-3}) is depicted in Figure **4**.

NaCl concentrations investigated in Figure **4** are twice lower than those of $CaCl_2$ and Na_2SO_4 for convenience since the plateau for which electrostatic interactions become negligible is reached with lower concentrations in the case of a salt containing only monovalent ions. In these three figures, it may be observed that the behavior with concentration differs depending on the valence of ions since electrostatic interaction are strongly affected by valence as it was previously highlighted. The divalent and large SO_4^{2-} co-ion is highly rejected even with a small membrane charge density when Ca^{2+} divalent counter-ion is less retained. However, the main difference between these three salts lies in the rejection evolution with concentration. Indeed, concentration increase tends to lower the salt rejection for NaCl and Na_2SO_4 (*i.e.* salts with a monovalent counter-ion and a mono- or divalent co-ion) due to the screening of membrane charge. Oppositely, a marked trend is obtained for $CaCl_2$ for which the higher valence of the counter-ion compared to that of the co-ion leads to the opposite behavior and rejection is found to increase with concentration.

This behavior observed for salts is more worthy of interest for ion mixtures since the impact of

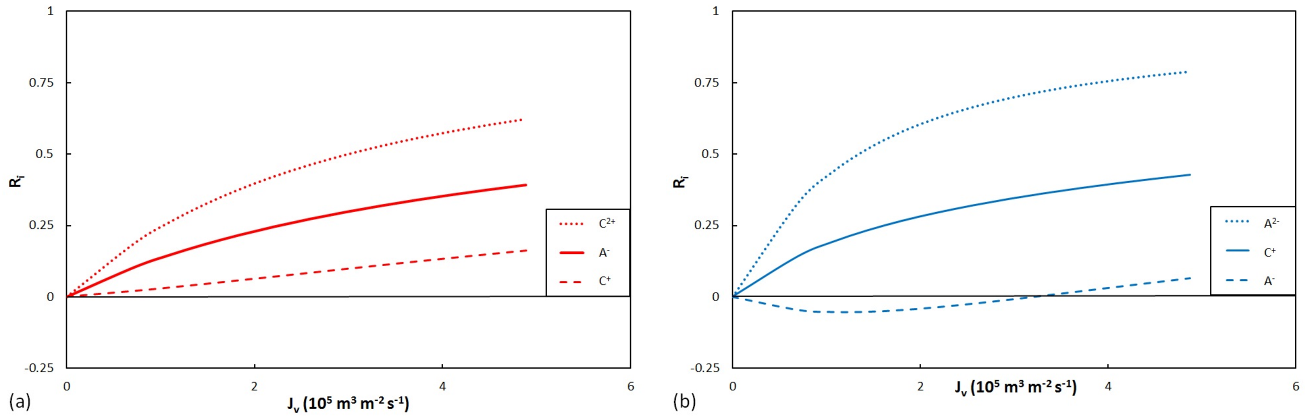

Figure 3: Evolution of ion rejection with permeation flux for a mixture containing a divalent cation (**3a**) and a divalent anion (**3b**) numerically obtained for a negative membrane charge and a “one-size-fits-all” for all ions.

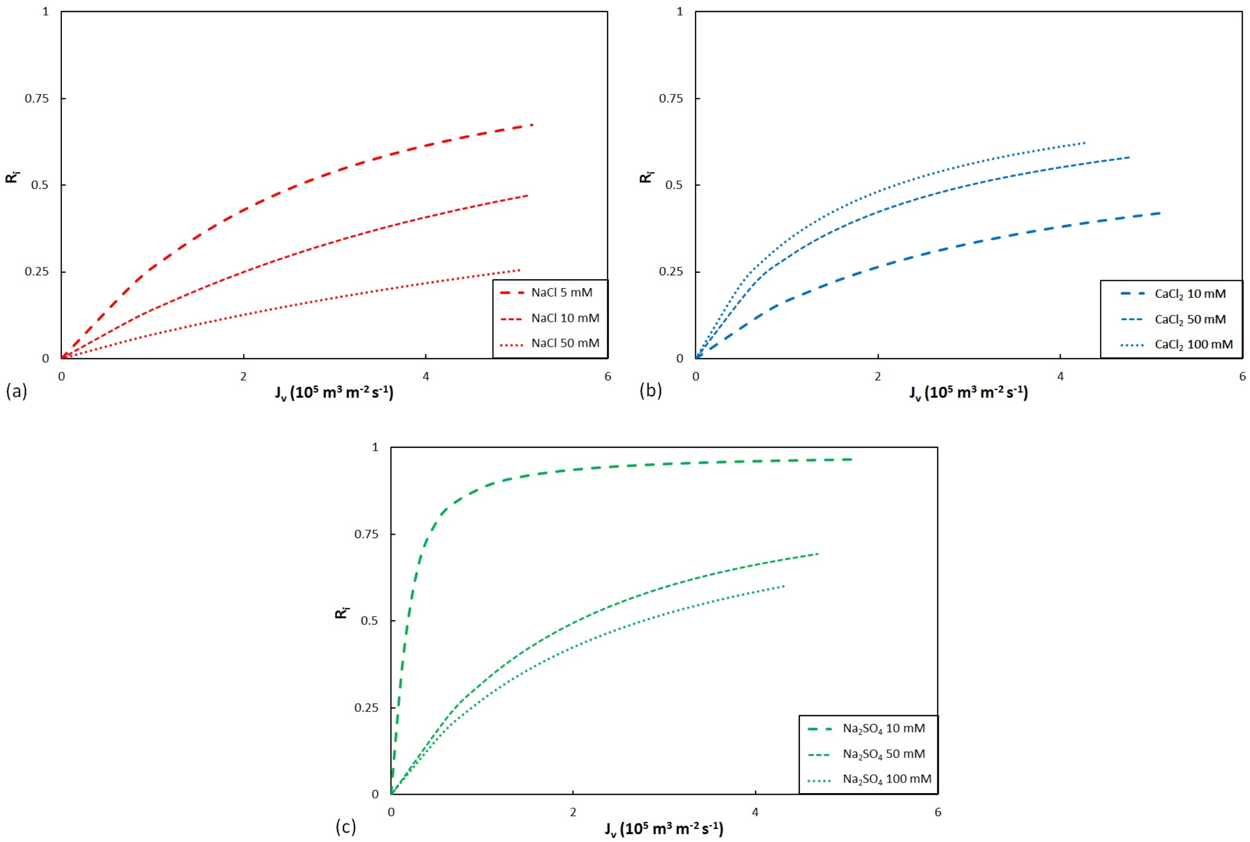

Figure 4: Evolution of salt rejection with permeation flux for various concentrations obtained numerically with NaCl (**4a**), $CaCl_2$ (**4b**) and Na_2SO_4 (**4c**).

concentration is different depending on the ion considered. For illustration purposes, Figure **5** depicts the influence of concentration on the rejection of three ions from a mixture.

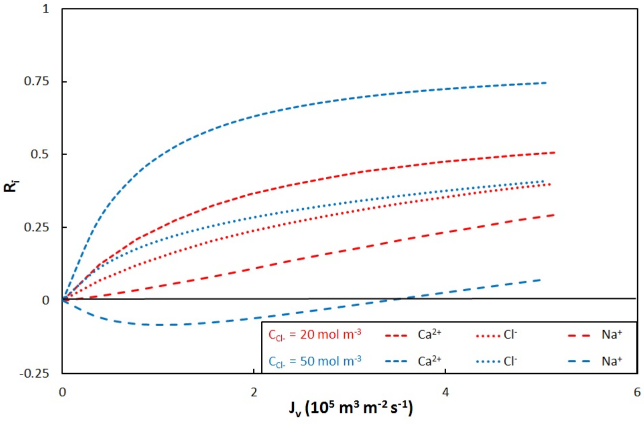

Figure 5: Evolution of ion rejection with permeation flux for two Cl^- concentrations (20 and 50 mol m^{-3}) obtained numerically for mixtures containing 66% of NaCl and 33%of $CaCl_2$.

As expected, concentration is found to have a strong influence on selectivity and Figure **5** shows that the selectivity between mono- and divalent ions strongly increases when concentration increases for the considered mixture. This figure shows that a decrease of electrostatic interactions (induced by concentration increase) tends to increase calcium rejection and chloride ions are therefore mainly transferred with sodium ions leading to lower rejection of the latter. It should be stressed that the behavior of selectivity with concentration differs depending on the ions present in the mixture and selectivity would evolve in another way if ions were different. In fact, electrostatic interactions are governed by the ratio of the membrane charge density to ion concentration, which means that a concentration increase has a similar impact as a decrease of the membrane charge. Finally, it should be noted that simulations provided in Figures **4** and **5** do not take variation of membrane charge density induced by an increase of the ionic strength into account and the membrane charge is considered identical for each simulation. Indeed, an increase in ionic strength (*i.e.* ion concentration) tends to collapse the Electrical Double Layer (EDL) at the membrane surface, which necessarily leads to a decrease of the zeta potential value but the increase of concentration can also lead to an increase of the membrane charge density by ion adsorption. It should also be mentioned that concentrations of the various species can have an influence on selectivity even for a neutral membrane (*i.e.* X_d = 0 mol m^{-3}) since transport of ions is also governed by electro-migration. This contribution to transport is indeed induced by the electrical potential gradient along the pore length that partially results from differences in ion diffusivities and is therefore sensitive to concentration.

A potential improvement of the discussion could be achieved by an experimental characterization of the membrane charge properties, for instance by streaming potential or current measurements [30-32].

3.4. Influence of Solution Confinement

Due to the narrow size of pores exhibited by nanofiltration membranes, solution inside pores is confined, leading to a modification of the physico-chemical properties of the solvent molecules. Indeed, the water molecules tend to be orientated by the presence of pore walls and electric potential gradient inside nanopores. The solvation energy barrier induced by this phenomenon at the membrane/solution interfaces strongly influences the rejection performances and it is included in the model by the Born relation through a decrease of the effective dielectric constant of the confined solution. The influence of the confinement (*i.e.* the decrease of dielectric constant) on salt rejection is shown in Figure **6**.

According to Born relation (Eq. 7), if the effective dielectric constant inside pores is lower than the bulk value ($\varepsilon_p < \varepsilon_b$), ion transfer into pores is thermodynamically unfavorable and rejection therefore increases, irrespective of ions considered. This means that ion or salt rejection should always be increased by water confinement inside pores. From Figure **6**, this is confirmed since ion rejection is found to be strongly increased by a decrease the dielectric constant of the confined solution. Moreover, this trend is particularly significant for divalent ions, which is mathematically obvious since solvation energy barrier is proportional to the square of the charge and repulsions are therefore necessarily stronger for multivalent ions. This strong impact of ε_p-value on rejection clearly complicates its determination for predictive modeling since a small uncertainty on this parameter can lead to tremendous mistakes on separation performances. That is why, experimental techniques devoted to accurate experimental characterization of ε_p-values can be relevant to discuss the physical meaning of this parameter [33, 34] but are not adequate for predictive purposes at the present time. It therefore seems that numerical assessment from rejections curves appears to be the best way [35, 36] even it requires many experimental data to be fully predictive.

CONCLUSION

Understanding of rejection mechanisms is known to be a primordial step when studying membrane processes. A classical transport model was used to discuss theoretical filtration performances for relevant study cases. This study has shown that the ion size has a noticeable influence of rejection and especially for ion mixtures but the choice of the size definition remains a major challenge that is not solved now. Influence of electrostatic interactions was also investigated through the influence of ion valence and concentration. First, ion valence was found to have a tremendous impact on performances. Indeed, it seems that rejection is always higher when valence is greater, especially when the co-ion valence is considered. Highest rejection was obtained when both co- and counter-ions have the uppermost valences. These theoretical trends should be tempered since valence is

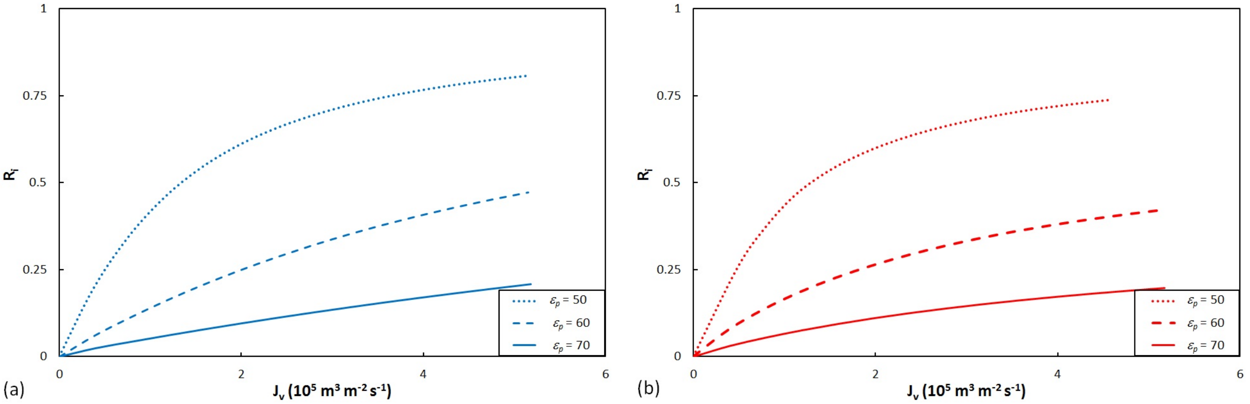

Figure 6: Evolution of rejection with permeation flux numerically predicted with three dielectric constants within the pores for NaCl (**6a**) and $MgCl_2$ (**6b**) at 50 mol m^{-3}.

never the sole difference between ions and differences in size and diffusivity also play a role in rejection. Additionally, this study showed that concentration has a varying influence on ion rejection depending on the valence of ions present in the solution and separation selectivity is therefore particularly sensitive to concentration variations. Finally, the water confinement induced by the nanoscale pore size was found to strongly increase the ion rejection irrespective of the ion considered.

ACKNOWLEDGMENT

The authors would like to thank the region of *Bourgogne-Franche-Comté* for its financial contribution to the project.

NOMENCLATURE

Latin Symbols

c_i	concentration of ion *i* within the pore (mol m^{-3})
$C_{i,p}$	permeate concentration of ion *i* (mol m^{-3})
$C_{i,r}$	bulk concentration of ion *i* (mol m^{-3})
D_i	molecular diffusion coefficient of ion i at infinite dilution (m^2 s^{-1})
F	Faraday constant (96487 C mol^{-1})
j_i	ionic flux of ion *i* (mol m^{-2} s^{-1})
J_v	volume permeation flux (m^3 m^{-2} s^{-1})
k_B	Boltzmann constant (1,38066.10^{-23} JK^{-1})
$K_{i,c}$	ionic hindrance factor for convection (dimensionless)
$K_{i,d}$	ionic hindrance factor for diffusion (dimensionless)
L_p	water permeability (m^3 m^{-2})
P	pressure (Pa)
r_i	radius of ion *i* (m)
R	universal gas constant (8.314 J mol^{-1} K^{-1})
R_i	rejection of ion *i* (dimensionless)
r_p	average pore radius (m)
T	temperature (K)
V	solvent velocity (m s^{-1})
X_d	effective membrane charge density (mol m^{-3})
z_i	valence of ion *i* (dimensionless)

Greek Symbols

γ_i	activity coefficient of ion *i* (dimensionless)
ΔP	applied pressure (Pa)
ΔW_i	solvation energy barrier (J)
$\Delta\psi_D$	Donnan potential (V)
$\Delta\pi$	osmotic pressure difference (Pa)
ε_0	permittivity of free space (8.85419 10^{-12}F m^{-1})
ε_b	bulk dielectric constant (dimensionless)
ε_p	pore dielectric constant (dimensionless)
η	dynamic viscosity (Pa s)
ϕ_i	steric partition coefficient (dimensionless)
ψ	electrical potential within the pore (V)
λ_i	ratio between ion and pore radii (dimensionless)

REFERENCES

[1] Afonso MD, Geraldes V, Rosa MJ, de Pinho MN. Nanofiltration removal of chlorinated organic compounds from alkaline bleaching effluents in a pulp and paper plant, Water Res 1992; 26: 1639-1643. https://doi.org/10.1016/0043-1354(92)90163-X

[2] Braeken L, Van der Bruggen B, Vandecasteele C, Regeneration of brewery waste water using nanofiltration, Water Res 2004; 38: 3075-3082. https://doi.org/10.1016/j.watres.2004.03.028

[3] Chakraborty S, Purkait MK, DasGupta S, De S, Basu JK. Nanofiltration of textile plant effluent for color removal and reduction in COD, Sep Purif Technol 2003; 31: 141-151. https://doi.org/10.1016/S1383-5866(02)00177-6

[4] Wang Z, Liu G, Fan Z, Yang X, Wang J, Wang S. Experimental study on treatment of electroplating wastewater by nanofiltration, J Membr Sci 2007; 305: 185-195. https://doi.org/10.1016/j.memsci.2007.08.011

[5] Déon S, Dutournié P, Limousy L, Bourseau P, Fievet P. Numerical Ways to Characterize the Deterioration of Nanofiltration Membranes, Int J Membr Sci Technol 2014; 1: 1-8. https://doi.org/10.15379/2410-1869.2014.01.01.1

[6] Bowen WR, Welfoot JS, Williams PM. Linearized transport model for nanofiltration: Development and assessment, American Institute of Chemical Engineering Journal 2002; 48: 760-773. https://doi.org/10.1002/aic.690480411

[7] Spiegler KS, Kedem O. Thermodynamics of hyperfiltration (Reverse Osmosis): Criteria for coefficient membranes, Desalination 1966; 1: 311-326. https://doi.org/10.1016/S0011-9164(00)80018-1

[8] Straatsma J, Bargeman G, van der Horst HC, Wesselingh JA, Can nanofiltration be fully predicted by a model?, J Membr Sci 2002; 198: 273-284. https://doi.org/10.1016/S0376-7388(01)00669-X

[9] Bouranene S, Fievet P, Szymczyk A. Investigating nanofiltration of multi-ionic solutions using the steric, electric and dielectric exclusion model, Chem Eng Sci 2009; 64: 3789-3798. https://doi.org/10.1016/j.ces.2009.05.020

[10] Cavaco Morão AI, Szymczyk A, Fievet P, Brites Alves AM. Modelling the separation by nanofiltration of a multi-ionic solution relevant to an industrial process, J Membr Sci 2008; 322: 320-330. https://doi.org/10.1016/j.memsci.2008.06.003

[11] Escoda A, Fievet P, Lakard S, Szymczyk A, Déon S. Influence of salts on the rejection of polyethyleneglycol by an NF organic membrane: Pore swelling and salting-out effects,

J Membr Sci 2010; 347: 174-182.
https://doi.org/10.1016/j.memsci.2009.10.021

[12] Déon S, Dutournié P, Limousy L, Bourseau P, Transport of salt mixtures through nanofiltration membranes: Numerical identification of electric and dielectric contributions, Sep. Purif Technol 2009; 69: 225-233.
https://doi.org/10.1016/j.seppur.2009.07.022

[13] Dutournié P, Limousy L, Déon S, Bourseau P. Unsteady transport of divalent salt through a mineral membrane of ultrafiltration: Numerical estimation of physical parameters, Desalination 2011; 265: 184-189.
https://doi.org/10.1016/j.desal.2010.07.050

[14] Gross RJ, Osterle JF. Membrane transport caracteristics of ultrafine capillaries, J Chem Phys 1968; 228: 49-234.

[15] Dresner L. Some remarks on the integration of extended Nernst-Planck equation in the hyperfiltration of multicomponent solutions, Desalination 1972; 10: 27-46.
https://doi.org/10.1016/S0011-9164(00)80245-3

[16] Schlögl R. Membrane permeation in system far from equilibrium, Berichte der Bunsengesellschaft Physik Chem 1966; 70: 400.

[17] Anderson JL, Quinn JA. Restricted transport in small pores: a model for steric exclusion and hindered particle motion, Biophys J 1974; 14: 130-150.
https://doi.org/10.1016/S0006-3495(74)70005-4

[18] Bungay PM, Brenner H. The motion of a closely-fitting sphere in a fluid-filled tube, Int J Multiphase Flow 1973; 1: 25.
https://doi.org/10.1016/0301-9322(73)90003-7

[19] Brenner H, Gaydos LJ. The constrained brownian movement of spherical particles in cylindrical pores of comparable radius, J Colloid Interface Sci 1977; 58: 312.
https://doi.org/10.1016/0021-9797(77)90147-3

[20] Ferry JD. Statistical evaluation of sieve constants in ultrafiltration, The Journal of General Physiology 1935; 20: 95-104.
https://doi.org/10.1085/jgp.20.1.95

[21] Bowen WR, Sharif AO. Transport through microfiltration membranes: particles hydrodynamics and flux reduction, J. Colloid Interface Sci 1994; 168: 414-421.
https://doi.org/10.1006/jcis.1994.1437

[22] Donnan FG. Theory of membrane equilibria and membrane potentials in the presence of non-dialysing electrolytes. A contribution to physical-chemical physiology, J Membr Sci 1995; 100: 45-55.
https://doi.org/10.1016/0376-7388(94)00297-C

[23] Born M. Volumen and hydratationswärme der ionen, Z. Physik Chem 1920; 1: 45-48.
https://doi.org/10.1007/bf01881023

[24] Guzman-Garcia AG, Pintauro PN, Verbrugge MW, Hill RF. Development of a space-charge transport model for ion-exchange membranes, AIChE J 1990; 36: 1061-1074.
https://doi.org/10.1002/aic.690360713

[25] Lide LR. Handbook of chemistry and physics, 79th Ed. ed., CRC Press, Boca Raton 1998.

[26] Dutournié P, Limousy L, Zouaoui N, Mahzoul H, Chevereau E. Facilitated transport of monovalent salt mixture through ultrafiltration Na-Mordenite membrane: Numerical investigations of electric and dielectric contributions, Desalination 2011; 280: 397-402.
https://doi.org/10.1016/j.desal.2011.07.027

[27] Déon S, Dutournié P, Limousy L, Bourseau P. The two-dimensional pore and polarization transport model to describe mixtures separation by nanofiltration: Model validation, AIChE J 2011; 57: 985-995.
https://doi.org/10.1002/aic.12330

[28] Hagmeyer G, Gimbel R. Modelling the rejection of nanofiltration membranes using zeta potential measurements, Sep Purif Technol 1999; 15: 19-30.
https://doi.org/10.1016/S1383-5866(98)00050-1

[29] Yaroshchuk A, Martìnez-Lladò X, Llenas L, Rovira M, de Pablo J. Solution-diffusion-film model for the description of pressure-driven trans-membrane transfer of electrolyte mixtures: One dominant salt and trace ions, J Membr Sci 2011; 368: 192-201.
https://doi.org/10.1016/j.memsci.2010.11.037

[30] Déon S, Escoda A, Fievet P. A transport model considering charge adsorption inside pores to describe salts rejection by nanofiltration membranes, Chem Eng Sci 2011; 66: 2823-2832.
https://doi.org/10.1016/j.ces.2011.03.043

[31] Fievet P, Sbai M, Szymczyk A, Vidonne A. Determining the [zeta]-potential of plane membranes from tangential streaming potential measurements: effect of the membrane body conductance, J Membr Sci 2003; 226: 227-236.
https://doi.org/10.1016/j.memsci.2003.09.007

[32] Yaroshchuk A, Ribitsch V, Role of channel wall conductance in the determination of z-potential from electrokinetic measurements, Langmuir 2002; 18: 2036-2038.
https://doi.org/10.1021/la015557m

[33] Bason S, Oren Y, Freger V. Characterization of ion transport in thin films using electrochemical impedance spectroscopy: II: Examination of the polyamide layer of RO membranes, J Membr Sci 2007; 302: 10-19.
https://doi.org/10.1016/j.memsci.2007.05.007

[34] Efligenir A, Fievet P, Déon S, Salut R. Characterization of the isolated active layer of a NF membrane by electrochemical impedance spectroscopy, J Membr Sci 2015; 477: 172-182.
https://doi.org/10.1016/j.memsci.2014.12.044

[35] Déon S, Escoda A, Fievet P, Dutournié P, Bourseau P. How to use a multi-ionic transport model to fully predict rejection of mineral salts by nanofiltration membranes, Chem Eng J 2012; 189-190: 24-31.
https://doi.org/10.1016/j.cej.2012.02.014

[36] Dutournié P, Limousy L, Zouaoui N, Mahzoul H, Chevereau E. Facilitated transport of monovalent salt mixture through ultrafiltration Na-Mordenite membrane: Numerical investigations of electric and dielectric contributions, Desalination 2011; 280: 397-402.
https://doi.org/10.1016/j.desal.2011.07.027.

Received on 11-12-2016 Accepted on 26-12-2016 Published on 31-12-2016

http://dx.doi.org/10.15379/2410-1869.2016.03.02.02